Contribution from the Laboratoire de Chimie Bioorganique et Bioinorganique, URA 1384, Université Paris-Sud XI, Bat. 420, 91405 Orsay, France, Institut für Physik, Medizinische Universität zu Lübeck, 2400 Lübeck, FRG, and Laboratoire de Chimie des Elêments de Transition, URA 419, Université Pierre et Marie Curie Paris VI, 4 Place Jussieu, 75005 Paris, France

Magnetic Susceptibility, EPR, Mössbauer, and X-ray Investigations of Heteropolynuclear Clusters Containing Iron(III) and Copper(II) Ions: $\{Cu(Mesalen)\}_2Fe(acac)(NO_3)_2$ and $\{Cu(Mesalen)\}_3Fe(acac)(PF_6)_2$†

Irène Morgenstern-Badarau,*[1a] Daniel Laroque,[1a] Eckhard Bill,[1b] Heiner Winkler,[1b] Alfred X. Trautwein,*[1b] Francis Robert,[1c] and Yves Jeannin[1c]

Received June 25, 1990

Magnetic susceptibility, EPR, Mössbauer, and X-ray studies have been performed on heteropolynuclear clusters containing iron(III) and copper(II) ions: $\{Cu(Mesalen)\}_2Fe(acac)(NO_3)_2$ and $\{Cu(Mesalen)\}_3Fe(acac)(PF_6)_2$ (Mesalen = 1,2-bis((methylsalicylidene)amino)ethane; acac = acetylacetonato(1-)). The spectroscopic results obtained for the trinuclear system {2CuFe} suggest strong antiferromagnetic coupling of iron(III) to the two copper(II) ions to yield a $S = {}^3/_2$ ground-state system. X-ray studies reveal that the tetranuclear system {3CuFe} crystallizes in the hexagonal space group $P6_122$ with $Z = 6$, $a = b = 14.471$ (3) Å, and $c = 50.372$ (2) Å; it consists of a trinuclear unit {2CuFe} plus a mononuclear Cu(Mesalen) molecule, arranged in helicoidal polymeric chains. Magnetic susceptibility, EPR, and Mössbauer studies under moderate fields consistently show that the {2CuFe} and Cu(Mesalen) moieties are weakly interacting. Under high-field and low-temperature conditions, this interaction is not observable in Mössbauer spectroscopy. Since the Mössbauer spectra under these conditions are identical for the tri- and tetranuclear clusters, we conclude that the {2CuFe} moieties are very similar in both cluster types. The presence of the additional Cu(Mesalen) molecule in the tetranuclear cluster expresses itself in the Mössbauer spectra only at elevated temperatures by an enhancement of the spin-spin relaxation rates of nearly 1 order of magnitude larger compared to the trinuclear cluster.

Introduction

Few heteropolynuclear molecules that contain spin-coupled iron(III) and copper(II) ions have been reported until now.[2] Within those studied so far, the focus has been on properties that are related to the antiferromagnetically coupled iron-copper pair of cytochrome *c* oxidase.[3] In addition to the current interest in analogue compounds for the redox center of the enzyme, such hetero di- and polynuclear systems display interesting magnetic properties dependent upon intramolecular and intermolecular interactions.[4]

To elucidate the magnetic properties, complementary methods such as magnetic susceptibility and Mössbauer and EPR spectroscopy may be applied to these systems. Magnetic susceptibility, EPR, and preliminary zero-field Mössbauer experiments of the trinuclear cluster $\{Cu(Mesalen)\}_2Fe(acac)(NO_3)_2$, noted as {2CuFe}, have been previously reported.[5] The temperature dependence of the effective magnetic moment over the temperature interval 4.2-300 K unambiguously demonstrates the presence of exchange coupling between the metal ions, with the two copper(II) ions ($S = {}^1/_2$) and the iron(III) ion ($S = {}^5/_2$) being antiferromagnetically coupled to a $S = {}^3/_2$ ground-state system. The EPR results at 4.2 K have been shown to be consistent with the magnetic susceptibility data, with the effective g values similar to those expected for a single-ion $S = {}^3/_2$ system subject to zero-field splitting of rhombic symmetry. The preliminary Mössbauer studies yielded unresolved hyperfine patterns, which suggested to us to perform a low-temperature, high-field investigation of the {2CuFe} complex.

Additionally, we have succeeded in the meantime in stabilizing the {2CuFe} complex in the solid state and we have obtained single crystals of a tetranuclear compound $\{Cu(Mesalen)\}_3Fe(acac)(PF_6)_2$, noted as {3CuFe}, which contains the trinuclear unit {2CuFe} packed within the crystallographic cell together with the monomer Cu(Mesalen). We now report on the X-ray crystal structure of this new {2CuFe}-containing system together with magnetic susceptibility, Mössbauer, and EPR investigations, and we compare the properties of the {2CuFe} and {3CuFe} systems.

Experimental Section

Synthesis. The synthesis of the complex {2CuFe} has been previously published.[5] The complex {3CuFe} was prepared from solutions of {2CuFe} in dichloromethane in presence of $NaPF_6$. {2CuFe} (0.002 mol) was dissolved in 500 mL of dichloromethane, and the solution was mixed with $NaPF_6$ (0.004 mol). The resulting dark purple solution was then

Table I. Crystallographic Data

formula	$(C_{59}H_{61}O_8N_6FeCu_3)_n(PF_6)_{2n}$
fw	1518.56
cryst system	hexagonal
space group	$P6_122$
$a = b$, Å	14.471 (3)
c, Å	50.372 (2)
V, Å^3	9135.2
Z	6
ρ(calcd), g cm^{-3}	1.66
cryst dimens, mm	0.35 × 0.22 × 0.18
$F(000)$	4644
system absences	$00l$; $l \neq 6n$
diffractometer	Enraf-Nonius CAD-4
radiation (graphite monochromator)	Mo Kα (λ = 0.71069 Å)
linear abs coeff, cm^{-1}	14.15
scan type	$\omega/2\theta$
scan range, deg	0.80 + 0.345 tan θ
θ limits, deg	1-23
octants collcd	$+h,+k,+l$
no. of data collcd	4856
no. of unique data collcd	2591
no. of unique data used	1933 (F_o)$^2 > 3\sigma(F_o^2)$)
decay, %	<1
$R = \sum(\|\|F_o\| - \|F_c\|\|)/\sum\|F_o\|$	4.78
$R_w = [\sum w(\|F_o\| - \|F_c\|)^2/\sum wF_o^2]^{1/2}$	5.31

† Abbreviations: Mesalen, 1,2-bis((methylsalicylidene)amino)ethane; acac, acetylacetonate(1-).

(1) (a) Université Paris-Sud XI. (b) Medizinische Universität zu Lübeck. (c) Université Pierre et Marie Curie Paris VI.
(2) (a) Gunter, M. J.; Mander, L. N.; Murray, K. S.; Clark, P. E. *J. Am. Chem. Soc.* **1981**, *103*, 6784-6787 and references within. (b) Dessens, S. E.; Merrill, C. L.; Saxton, R. J.; Ilaria, R. L.; Lindsey, J. W.; Wilson, L. J. *J. Am. Chem. Soc.* **1982**, *104*, 4357-4361. (c) Serr, B. R.; Headford, E. L.; Elliot, C. M.; Anderson, O. P. *J. Chem. Soc., Chem. Commun.* **1988**, 92-94. (c) Koch, C. A.; Reed, C. A.; Brewer, G. A.; Rath, N. P.; Scheidt, W. R.; Gupta, G.; Lang, G. *J. Am. Chem. Soc.* **1989**, *111*, 7645-7648.
(3) (a) Tweedle, M. F.; Wilson, L. J.; Garcia-Iniguez, L.; Babcock, G. T.; Palmer, G. *J. Biol. Chem.* **1978**, *253*, 8065. (b) Moss, T. H.; Shapiro, E.; King, T. E.; Beinert, H.; Hartzell, C. *J. Biol. Chem.* **1978**, *258*, 8543. (c) Malmström, B. G. In *Metal Ion Activation of Dioxygen*; Spiro, T. G., Ed.; Wiley: New York, 1980. (d) Widström, M.; Krab, K.; Saraste, M. *Cytochrome Oxidase: A synthesis*; Academic Press: New York/London, 1981. (e) Brudwig, G. W.; Stevens, T. H.; Morse, R. H.; Chan, S. I. *Biochemistry* **1981**, *20*, 3912-3921.
(4) See for example: (a) Griffith, J. S. *Mol. Phys.* **1971**, *21*, 141-143. (b) Blake, A. B.; Yavati, A.; Hatfield, W. E.; Sethulekshmi, C. N. *J. Chem. Soc., Dalton Trans.* **1985**, 2509-2520.

0020-1669/91/1330-3180$02.50/0

Table II. Atomic Fractional Coordinates

attom	x/a	y/b	z/c	U(eqv),[a] Å²
Fe(1)	0.5106 (2)	0.0000	0.0000	0.0319
Cu(1)	0.4204 (1)	0.1059 (1)	0.03518 (3)	0.0354
O(1)	0.5541 (6)	0.1396 (6)	0.0182 (1)	0.0318
C(1)	0.635 (1)	0.2404 (9)	0.0170 (2)	0.0340
C(2)	0.740 (1)	0.256 (1)	0.0161 (2)	0.0419
C(3)	0.827 (1)	0.359 (1)	0.0137 (2)	0.0440
C(4)	0.813 (1)	0.446 (1)	0.0127 (3)	0.0505
C(5)	0.712 (1)	0.433 (1)	0.0130 (2)	0.0449
C(6)	0.6205 (9)	0.3308 (8)	0.0151 (2)	0.0325
C(7)	0.515 (1)	0.322 (1)	0.0147 (2)	0.0355
N(8)	0.4339 (8)	0.2410 (8)	0.0249 (2)	0.0373
C(9)	0.326 (1)	0.231 (1)	0.0233 (3)	0.0399
C(10)	0.505 (1)	0.411 (1)	0.0021 (2)	0.0449
O(11)	0.3928 (6)	−0.0359 (7)	0.0278 (1)	0.0409
C(11)	0.313 (1)	−0.1263 (9)	0.0389 (2)	0.0347
C(12)	0.330 (1)	−0.212 (1)	0.0422 (2)	0.0411
C(13)	0.250 (1)	−0.306 (1)	0.0543 (2)	0.0497
C(14)	0.155 (1)	−0.316 (1)	0.0630 (3)	0.0566
C(15)	0.137 (1)	−0.228 (1)	0.0597 (2)	0.0574
C(16)	0.217 (1)	−0.131 (1)	0.0468 (2)	0.0394
C(17)	0.193 (1)	−0.042 (1)	0.0457 (3)	0.0416
N(18)	0.2711 (8)	0.0549 (8)	0.0437 (2)	0.0426
C(19)	0.256 (1)	0.148 (1)	0.0450 (3)	0.0466
C(20)	0.079 (1)	−0.068 (1)	0.0488 (3)	0.0599
O(21)	0.5832 (7)	−0.0509 (7)	0.0239 (1)	0.0436
C(22)	0.673 (1)	−0.043 (1)	0.0215 (3)	0.0387
C(23)	0.739 (1)	0.0000	0.0000	0.0484
C(24)	0.703 (1)	−0.094 (1)	0.0444 (3)	0.0653
O(24)	0.4969 (7)	0.1555 (7)	0.0778 (2)	0.0451
Cu(2)	0.6022 (2)	0.30110 (9)	0.0833	0.0455
C(25)	0.502 (1)	0.076 (1)	0.0896 (2)	0.0416
C(26)	0.403 (1)	−0.018 (1)	0.0949 (2)	0.0494
C(27)	0.400 (1)	−0.107 (1)	0.1066 (2)	0.0541
C(28)	0.498 (2)	−0.103 (1)	0.1133 (3)	0.0658
C(29)	0.594 (1)	−0.013 (1)	0.1080 (3)	0.0633
C(30)	0.600 (1)	0.080 (1)	0.0966 (3)	0.0513
C(31)	0.705 (1)	0.173 (1)	0.0914 (3)	0.0572
N(32)	0.7163 (9)	0.266 (1)	0.0871 (2)	0.0574
C(33)	0.824 (1)	0.360 (1)	0.0826 (3)	0.0677
C(34)	0.804 (1)	0.159 (2)	0.0921 (4)	0.0844
P(1)	1.0571 (3)	0.2610 (4)	0.02477 (9)	0.0627
F(1)	1.089 (1)	0.382 (1)	0.0288 (4)	0.130 (8)*
F(2)	0.959 (1)	0.222 (2)	0.0439 (3)	0.15 (1)*
F(3)	0.986 (1)	0.253 (2)	−0.0003 (3)	0.137 (8)*
F(4)	1.158 (1)	0.301 (2)	0.0048 (3)	0.131 (8)*
F(5)	1.030 (1)	0.142 (1)	0.0193 (4)	0.127 (9)*
F(6)	1.132 (1)	0.270 (1)	0.0489 (3)	0.080 (5)*
F(101)	1.182 (1)	0.337 (2)	0.0253 (5)	0.17 (1)*
F(102)	1.043 (2)	0.348 (1)	0.0429 (3)	0.108 (8)*
F(103)	0.930 (1)	0.190 (1)	0.0257 (4)	0.105 (7)*
F(104)	1.048 (2)	0.318 (2)	−0.0014 (3)	0.110 (8)*
F(105)	1.063 (2)	0.209 (2)	0.0524 (3)	0.115 (8)*
F(106)	1.065 (1)	0.174 (1)	0.0089 (3)	0.089 (7)*

[a] Asterisk indicates isotropic U.

heated and stirred for 2 h at 40 °C. The solution was kept to slow evaporation at room temperature. After 3 days, dark black crystals as hexagonal prisms were obtained. Anal. Calc for $C_{59}H_{61}N_6O_8P_2F_{12}Cu_3Fe$: C, 46.6; H, 4.02; N, 5.53; P, 4.08; Cu, 12.55; Fe, 3.68. Found: C, 45.55; H, 4.02; N, 5.19; P, 4.06; Cu, 12.26; Fe, 3.65.

X-ray Data Collection and Structure Solution. A dark parallelepipedic crystal was mounted on a CAD4 Enraf Nonius automatic diffractometer. The unit cell constants were refined from 25 centered reflections ($6.34° < \theta < 12.73°$). The intensities of 4856 reflections were collected in the θ–2θ scan mode up to $2\theta_{max} = 46°$. Among them, 2591 independent reflections were merged (merging factor 0.036). A total of 1933 reflections with $I > 3\sigma(I)$ were kept for further calculations. They were corrected for Lorentz and polarization factors and for absorption (DIFABS).[6] The crystallographic data are summarized in Table I.

The structure was solved by direct methods (SHELXS-86)[7] and successive Fourier syntheses. The atomic coordinates were refined by full-matrix least-squares methods ($w = 1.0$). As the PF_6 group was found disordered, restraints were applied on P–F bonds and F–P–F angles. All the thermal parameters were made anisotropic except the fluorine atoms, which were kept isotropic (Table S1 of the supplementary material). All

Table III. Selected Interatomic Distances (Å) and Bond Angles (deg)

Distances			
Fe(1)–Cu(1)	3.033 (2)	C(13)–C(14)	1.37 (2)
Fe(1)–O(1)	2.013 (7)	C(14)–C(15)	1.44 (2)
Fe(1)–O(11)	2.060 (8)	C(15)–C(16)	1.45 (2)
Fe(1)–O(21)	1.967 (8)	C(16)–C(17)	1.48 (2)
Cu(1)–O(1)	1.940 (7)	C(17)–N(18)	1.29 (2)
Cu(1)–N(8)	1.94 (1)	C(17)–C(20)	1.51 (2)
Cu(1)–O(11)	1.923 (8)	N(18)–C(19)	1.48 (2)
Cu(1)–N(18)	1.95 (1)	O(21)–C(22)	1.26 (1)
Cu(1)–O(24)	2.357 (8)	C(22)–C(23)	1.37 (2)
O(1)–C(1)	1.34 (1)	C(22)–C(24)	1.54 (2)
C(1)–C(2)	1.42 (2)	O(24)–Cu(2)	1.905 (8)
C(1)–C(6)	1.43 (2)	O(24)–C(25)	1.33 (1)
C(2)–C(3)	1.39 (2)	Cu(2)–N(32)	1.96 (1)
C(3)–C(4)	1.38 (2)	C(25)–C(26)	1.42 (2)
C(4)–C(5)	1.37 (2)	C(25)–C(30)	1.43 (2)
C(5)–C(6)	1.41 (2)	C(26)–C(27)	1.40 (2)
C(6)–C(7)	1.47 (2)	C(27)–C(28)	1.43 (2)
C(7)–N(8)	1.28 (1)	C(28)–C(29)	1.37 (2)
C(7)–C(10)	1.50 (2)	C(29)–C(30)	1.43 (2)
N(8)–C(9)	1.49 (1)	C(30)–C(31)	1.47 (2)
C(9)–C(19)	1.56 (2)	C(31)–N(32)	1.29 (2)
O(11)–C(11)	1.36 (1)	C(31)–C(34)	1.54 (2)
C(11)–C(12)	1.39 (2)	N(32)–C(33)	1.48 (2)
C(11)–C(16)	1.41 (2)	C(33)–C(33)	1.49 (3)
C(12)–C(13)	1.42 (2)		
Angles			
O(1)–Fe(1)–O(1)	158.1 (4)	C(16)–C(11)–C(12)	122.5 (11)
O(11)–Fe(1)–O(1)	75.4 (3)	C(13)–C(12)–C(11)	119.4 (13)
O(11)–Fe(1)–O(1)	89.2 (3)	C(14)–C(13)–C(12)	121.8 (13)
O(11)–Fe(1)–O(11)	91.0 (5)	C(15)–C(14)–C(13)	118.8 (13)
O(21)–Fe(1)–O(1)	98.0 (3)	C(16)–C(15)–C(14)	120.2 (14)
O(21)–Fe(1)–O(1)	97.7 (3)	C(15)–C(16)–C(11)	117.2 (12)
O(21)–Fe(1)–O(11)	91.1 (3)	C(17)–C(16)–C(11)	126.8 (11)
O(21)–Fe(1)–O(11)	172.7 (3)	C(17)–C(16)–C(15)	115.7 (12)
O(21)–Fe(1)–O(21)	87.7 (5)	N(18)–C(17)–C(16)	119.2 (12)
N(8)–Cu(1)–O(1)	92.5 (4)	C(20)–C(17)–C(16)	118.8 (12)
O(11)–Cu(1)–O(1)	80.3 (3)	C(20)–C(17)–N(18)	121.8 (13)
O(11)–Cu(1)–N(8)	152.7 (4)	C(17)–N(18)–Cu(1)	128.8 (9)
N(18)–Cu(1)–O(1)	165.6 (4)	C(19)–N(18)–Cu(1)	108.0 (8)
N(18)–Cu(1)–N(8)	88.5 (4)	C(19)–N(18)–C(17)	122.9 (11)
N(18)–Cu(1)–O(11)	92.3 (4)	N(18)–C(19)–C(9)	109.1 (10)
O(24)–Cu(1)–O(1)	93.8 (3)	C(22)–O(21)–Fe(1)	129.2 (9)
O(24)–Cu(1)–N(8)	98.2 (4)	C(23)–C(22)–O(21)	124.7 (14)
O(24)–Cu(1)–O(11)	108.5 (3)	C(24)–C(22)–O(21)	114.5 (13)
O(24)–Cu(1)–N(18)	100.2 (4)	C(24)–C(22)–C(23)	120.7 (13)
Cu(1)–O(1)–Fe(1)	100.2 (3)	C(22)–C(23)–C(22)	124.3 (18)
C(1)–O(1)–Fe(1)	137.1 (7)	Cu(2)–O(24)–Cu(1)	117.7 (4)
C(1)–O(1)–Cu(1)	121.1 (7)	C(25)–O(24)–Cu(1)	111.4 (7)
C(2)–C(1)–O(1)	117.7 (10)	C(25)–O(24)–Cu(2)	122.0 (8)
C(6)–C(1)–O(1)	123.0 (11)	N(32)–Cu(2)–O(24)	92.4 (4)
C(6)–C(1)–C(2)	119.2 (11)	N(32)–Cu(2)–O(24)	165.7 (4)
C(3)–C(2)–C(1)	120.1 (12)	N(32)–Cu(2)–N(32)	86.3 (8)
C(4)–C(3)–C(2)	120.5 (13)	C(26)–C(25)–O(24)	116.0 (13)
C(5)–C(4)–C(3)	120.6 (13)	C(30)–C(25)–O(24)	123.8 (13)
C(6)–C(5)–C(4)	121.8 (12)	C(30)–C(25)–C(26)	120.2 (13)
C(5)–C(6)–C(1)	117.9 (11)	C(27)–C(26)–C(25)	120.3 (15)
C(7)–C(6)–C(1)	123.3 (10)	C(28)–C(27)–C(26)	119.5 (16)
C(7)–C(6)–C(5)	118.8 (11)	C(29)–C(28)–C(27)	120.2 (15)
N(8)–C(7)–C(6)	120.5 (11)	C(30)–C(29)–C(28)	121.9 (16)
C(10)–C(7)–C(6)	118.5 (11)	C(29)–C(30)–C(25)	117.8 (15)
C(10)–C(7)–N(8)	121.0 (11)	C(31)–C(30)–C(25)	123.3 (13)
C(7)–N(8)–Cu(1)	128.1 (9)	C(31)–C(30)–C(29)	118.8 (15)
C(9)–N(8)–Cu(1)	110.0 (8)	N(32)–C(31)–C(30)	121.0 (14)
C(9)–N(8)–C(7)	120.1 (11)	C(34)–C(31)–C(30)	118.8 (15)
C(19)–C(9)–N(8)	106.9 (10)	C(34)–C(31)–N(32)	120.1 (15)
Cu(1)–O(11)–Fe(1)	99.1 (4)	C(31)–N(32)–Cu(2)	127.1 (11)
C(11)–O(11)–Fe(1)	136.3 (8)	C(33)–N(32)–Cu(2)	112.3 (10)
C(11)–O(11)–Cu(1)	124.5 (7)	C(33)–N(32)–C(31)	120.4 (13)
C(12)–C(11)–O(11)	117.2 (11)	C(33)–C(33)–N(32)	112.6 (9)
C(16)–C(11)–O(11)	120.4 (11)		

(5) Morgenstern-Badarau, I.; Wickman, H. H. *Inorg. Chem.* **1985**, *24*, 1889–1892.
(6) Stuart, D.; Walker, N. *Acta Crystallogr.* **1983**, *139*, 158.
(7) Sheldrick, G. M. A program for crystal structure determination. University of Goettingen, Goettingen, FRG, 1986.

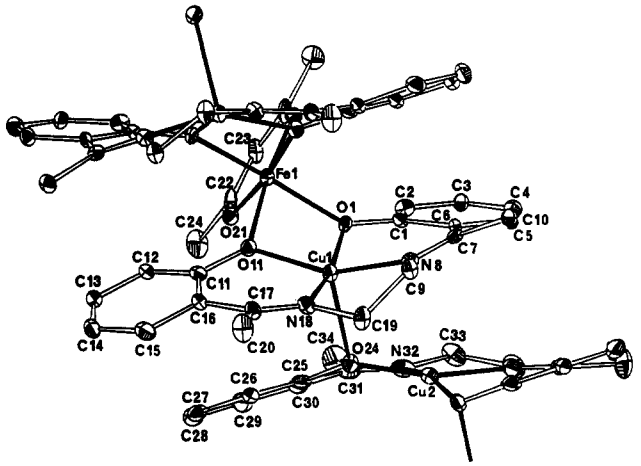

Figure 1. ORTEP drawing of the {3CuFe} asymmetric unit, showing the 50% probability thermal ellipsoids and the atom-numbering scheme.

the hydrogen atoms were found on difference Fourier maps but not introduced in the refinement. The anomalous part of the scattering factors was used. All calculations were performed on the micro-VAX computer of the laboratory using the crystallographic program CRYSTALS.[8] The final atomic coordinates are listed in Table II, and the interatomic distances and bond angles are in Table III and Table S2 of the supplementary material for the PF_6 group.

Magnetic Measurements. The experiments utilized a variable-temperature (4.2–300 K) Faraday type magnetometer equipped with an Oxford Instruments continuous-flow cryostat. Polycrystalline samples weighing about 4 mg were obtained from pulverized crystals. The susceptibility data were corrected for diamagnetism, estimated at -850×10^{-6} cm^3/mol. The fittings to the experimental data were carried out by minimizing the R factor defined as $R = \sum[\chi_M^{obs} - \chi_M^{calc}]^2/\sum[\chi_M^{obs}]^2$, according to least-squares minimization procedures.

EPR Spectroscopy. Measurements on pulverized crystals were performed at X-band frequency, using a Bruker ER-200D spectrometer, equipped with an Oxford Instruments continuous-flow cryostat (4.2–300 K). The magnetic field was determined with a Hall probe, and the klystron frequency, with a Hewlett-Packard frequency meter.

Mössbauer Spectroscopy. The Mössbauer spectrometer worked in the conventional constant-acceleration mode with a source of 1.85 GBq ^{57}Co/Rh (Amersham Buchler). From calibration measurements we get a standard line width of 0.23 mm s^{-1}. Isomer shifts are given relative to metallic iron (α-iron) at room temperature. The Mössbauer cryostats consisted of a helium-bath cryostat (MD 306, Oxford Instruments) and a superconducting magnet system with split coil geometry (Oxford Instruments). The γ-beam could be transmitted parallel or perpendicular to the field. The sample temperature in the cryomagnet was regulated independently from the source temperature in a variable-temperature insert. Small fields of 20 mT could be applied to the tail of the bath cryostat with the help of a permanent magnet.

Results and Discussion

Structure. The cation $\{[Cu(Mesalen)]_3Fe(acac)\}^{2+}$ of the {3CuFe} system has a polymeric structure. The asymmetric unit is formed by a trinuclear $[Cu(Mesalen)]_2Fe(acac)$ unit plus a Cu(Mesalen) unit. These asymmetric units are related one to the other by binary axes passing respectively through the Fe(1) or the Cu(2) atoms (Figure 1).

The trinuclear unit $[Cu(Mesalen)]_2Fe(acac)$ shows a nearly regular octahedral coordination of the iron, achieved by oxygen donor atoms from one acac and two Cu(Mesalen) molecules acting as ligands, identical with the previously expected structure.[5] The Fe–O(21) distance (1.967 Å) is similar to the one observed in the regular octahedron of the $Fe(acac)_3$ complex[9] (1.95 Å). The two other distances appear longer and different, with Fe–O(1) equal to 2.013 Å and Fe–O(11) equal to 2.060 Å, resulting in an elongation of the octahedron along the direction O(11′)–Fe–O(11).

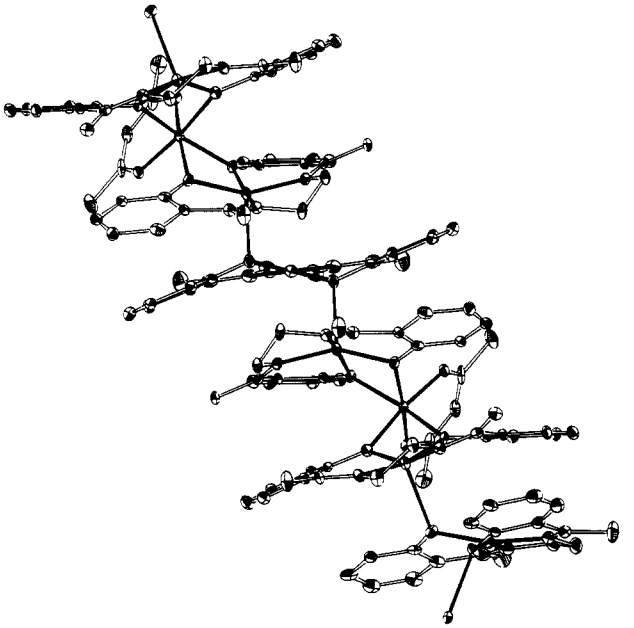

Figure 2. Fragment of the polymeric chain showing the "copper–iron–copper–copper" sequence.

Such an inequivalence of the two bonds provided by the phenolic oxygen atoms of the Schiff-base complex has been observed in heterodinuclear Cu(II)–M(II) molecules of adduct type,[10] in which the Cu(salen) molecule achieved the octahedral coordination of a divalent ion. A noteworthy feature is the nonusual dihedral angle (11.4°) between the two Cu(Mesalen) molecules, which are expected to be orthogonal in the free trinuclear unit. This is due to the steric hindrance induced by the fifth coordination of the copper ion of the trinuclear unit to the phenolic oxygen of the copper mononuclear unit. The resulting effect is a folding of the Cu(Mesalen) ligand around the O(1)O(11) axis (the angle between the Fe(1)O(1)O(11) plane and the O(1)O(11)N(8)N(18) plane is 36.6°). This fifth coordination also corresponds to a long copper–oxygen distance Cu(1)–O(24) equal to 2.357 Å compared to the Cu(1)–O(1) and Cu(1)–O(11) bonds (1.940 and 1.923 Å). The mononuclear unit with its four-coordinated copper atom is related to two different trinuclear units via oxygen atoms O(24) and O(24′).

In such a way, a metallic chain shown in Figure 2 is formed through a sequence that is Cu(1′),Fe(1),Cu(1),Cu(2) with distances Fe(1)–Cu(1) and Cu(1)–Cu(2), respectively, equal to 3.033 (2) and to 3.654 (2) Å. The corresponding angles are Cu(1′)–Fe(1)–Cu(1) equal to 93.8 (8)°, Fe(1)–Cu(1)–Cu(2) equal to 116.94 (6)°, and Cu(1)–Cu(2)–Cu(1) equal to 102.85 (7)°.

The Mesalen moiety of the trinuclear unit adopts the well-known umbrella conformation[11] with a γ dihedral angle between the two phenolate rings equal to 19.6° and with angles between these two planes and the mean O2N2 plane, α and β, equal to 15.2 and 8.0°, respectively. The relation $\gamma \cong \alpha + \beta$ confirms the umbrella shape, which, in the case of pentacoordinate species, is preferred to the planar conformation. In the mononuclear unit, the two phenolate rings are nearly parallel with a distance between the two planes of 0.68 Å. The ligand adopts a stepped conformation, instead of the planar one observed in four-coordinate complexes, due to the bonding of each phenolic oxygen O(24) and O(24′) to the copper ion of two different trinuclear units.

In the crystal the helicoidal polymeric chains are parallel, leaving free space for the PF_6 anions without too close contacts

(8) Watkin, D. J.; Carruthers, J. R.; Betteridge, P. W. Crystals user guide. University of Oxford, Oxford, U.K., 1985.
(9) Roof, R. B. *Acta Crystallogr.* **1956**, *9*, 781–786.
(10) (a) O'Bryan, N. B.; Maier, T. O.; Paul, I. C.; Drago, R. S. *J. Am. Chem. Soc.* **1973**, *95* (20), 6640–6643. (b) Fenton, D. E.; Bresciani-Pahor, N.; Calligaris, M.; Nardin, G.; Randaccio, L. *J. Chem. Soc., Chem. Commun.* **1979**, 39–40. (c) O'Connor, C. J.; Freyberg, D. P.; Sinn, E. *Inorg. Chem.* **1979**, *18*, 1077–1088.
(11) Calligaris, M.; Nardin, G.; Randaccio, L. *Coord. Chem. Rev.* **1972**, *7*, 385–403.

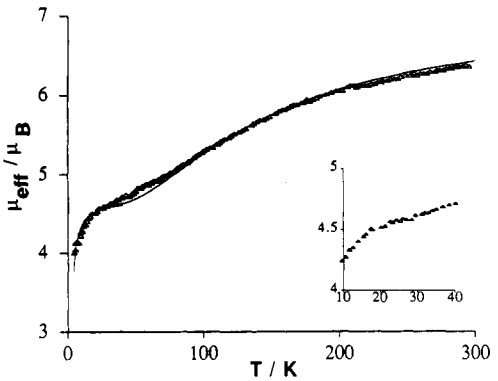

Figure 3. Effective magnetic moment data for {3CuFe} over the temperature range 4.2–300 K. The solid lines are the fit of the susceptibility equations derived from two different models successively in the high- and low-temperature ranges. The overlap of the solid lines is obtained over 10 K (30–40 K).

between the metallic sites of the cations.

Magnetic Properties. The magnetic susceptibility data of the {3CuFe} system are shown in Figure 3 in the form of the molecular effective magnetic moment (μ_{eff} in μ_B units) versus the temperature in the range 4.2–300 K. A continuous decrease is observed from 6.34 μ_B at room temperature to 3.98 μ_B at 4.2 K. While the sample is cooled, changes in the curvature are observed at around 40 K (μ_{eff} = 4.72 μ_B) and then at 30 K (μ_{eff} = 4.62 μ_B). Within this interval, the decrease is smaller than at higher or lower temperatures.

In order to interpret the magnetic data, we have considered separately the high- and the low-temperature ranges, 300–30 and 40–4.2 K, respectively, with an overlap of 10 K between the two ranges, which corresponds to the approximate plateau of the experimental data. The models we used have been deduced from consideration of the crystal structure, from our previous results related to the trinuclear complex[5] and from complementary data provided by EPR and Mössbauer spectroscopies.

Magnetic Study in the 300–30 K Range. Although the crystal structure suggests a polymeric chain formed by the succession of {Cu–Fe–Cu–Cu} sequences, it also shows that weak interunit interaction, compared with the intramolecular interaction in the trinuclear entity, can be predicted from the relative disposition of the two molecular units {2CuFe} and Cu(Mesalen). Indeed, the d orbital of the copper ion in Cu(Mesalen), which contains the unpaired electron pointing toward the nearest neighbors, i.e. the phenolic oxygen and imine nitrogen atoms of the salen ligand, presents, on the one hand, a δ overlap with the corresponding copper d orbital in the trinuclear entity. On the other hand, the p orbital of the phenolic oxygen providing a route for the exchange is orthogonal to both of these d orbitals. Such disposition is also found in several salen complexes, which are very weakly coupled dimers in the solid state.[11,12] Any efficient exchange pathway is ruled out: the interunit interaction, if any, must be much smaller than the intramolecular exchange of the trinuclear entity, found previously equal to −63 cm^{-1} in the free complex.[5] Therefore, in the range 300–30 K, we have neglected any interunit coupling and, supposing the two molecular {2CuFe} and Cu(Mesalen) units were independent, we have taken the magnetic behavior as the sum

$$\chi_{\{3CuFe\}} = \chi_{\{2CuFe\}} + \chi_{Cu(Mesalen)} \quad (1)$$

We have deduced[5] $\chi_{\{2CuFe\}}$ from perturbation theory after considering the exchange interaction as the leading term, characterized by an equivalent coupling parameter J between the iron(III) ion and the two copper(II) ions, and neglecting the copper–copper interaction ($J' \sim 0$), according to diagram I.

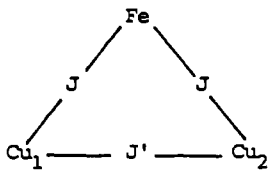

diagram I

The eigenvalues of the exchange Hamiltonian

$$\mathcal{H}_{exch} = -J_{\{2CuFe\}}(\mathcal{S}_{Cu1}\mathcal{S}_{Fe} + \mathcal{S}_{Cu2}\mathcal{S}_{Fe}) \quad (2)$$

are shown schematically in diagram II, and the interaction is

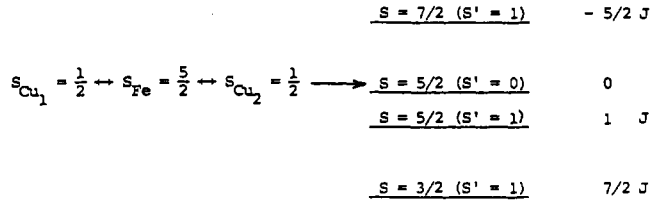

diagram II

supposed antiferromagnetic. Two additional terms are then required for a given manifold S:

$$\mathcal{H}_{cf} + \mathcal{H}_{Zeeman} = \mathcal{S}(D)\mathcal{S} + \beta H(g)\mathcal{S} \quad (3)$$

Here D parametrizes the zero-field splitting and g has the usual meaning. If the same g value is taken for all the manifolds and if the temperature is large compared with the zero-field splitting, the derived susceptibility expression is

$$\chi_{\{2CuFe\}} = (N\mu_B^2/kT)(g^2/4) \times \frac{35 + 35\exp(-J/kT) + 10\exp(-7J/kT) + 84\exp(5J/2kT)}{3 + 3\exp(-J/kT) + 2\exp(-7J/kT) + 4\exp(5J/2kT)} \quad (4)$$

The monomeric copper susceptibility is given by the well-known Curie law for $S = {}^1/_2$ systems:

$$\chi_{Cu(Mesalen)} = (N\mu_B^2/kT)(g^2/4) \quad (5)$$

The fit of the high-temperature susceptibility data with the sum of the two molecular susceptibility contributions (eqs 4 and 5) provides the following parameters:

$$J_{\{2CuFe\}} = -52.6\ cm^{-1} \qquad g_{\{2CuFe\}} = 2.15 \qquad g_{Cu(Mesalen)} = 2.24$$

$$R \text{ factor} = 7 \times 10^{-5}$$

These values can be compared with those corresponding to isolated molecules. For the trinuclear complex, the previously obtained values[5] were equal to J = −63 cm^{-1} and g = 2.08. In the tetranuclear system, the new results for {2CuFe} are slightly different: the observed differences are probably due to the constraints provided by the presence of the additional stacked copper molecule, as reported in the structure description, which induces subtle changes in metallic site symmetries. The g factor for the Cu(Mesalen) moiety is also slightly different from the one of the free Cu(Mesalen) complex, which we recorded by EPR methods (g_{mean} = 2.15), probably because of analogous solid-state constraints.

Magnetic Study in the 40–4.2 K Range. In the 40–4.2 K temperature range, two possible effects that are of the order of magnitude of the Boltzmann energy can affect the temperature dependence of the effective magnetic moment, i.e. weak interaction between the two entities and zero-field splitting of populated states. EPR spectroscopy confirms that some interaction is effective, since at X-band frequency no spectrum can be recorded. In addition, we already know from the previous {2CuFe} experiments[5] that its $S = {}^3/_2$ ground state, being well separated from the excited state,

(12) Baker, E. N.; Hall, D.; McKinnon, A. J.; Waters, T. N. *Chem. Commun.* **1967**, 134.

is the only one populated below 30 K. Then interunit interactions, detectable at low temperature, occur between the trinuclear molecules in their ground state, $S = {}^3/_2$, and the $S = {}^1/_2$ mononuclear copper molecules. Furthermore, from the Mössbauer experiments (see below), at 1.5 K and under moderate field, an antiferromagnetic interaction of magnitude 1.6 cm^{-1} has been found between the two moieties in their $S = {}^3/_2$ and $S = {}^1/_2$ ground states. All these results corroborate the fact that coupling between the two moieties has to be taken into account in the interpretation of the low-temperature magnetic data.

The problem we then have to discuss, considering all statements from above, is how to handle such coupling in the most probable realistic way, since to the best of our knowledge, no model exists to date that deals with interactions related to a polymeric chain containing the spin sequence "${}^1/_2$–${}^5/_2$–${}^1/_2$–${}^1/_2$".

Relying on the Mössbauer study on the one hand and on the structural arrangement on the other hand, we have considered two interactions: an intracluster interaction between the two $S = {}^3/_2$ and $S = {}^1/_2$ moieties and an intercluster interaction between the tetranuclear units, each of them being surrounded by two identical neighbors. The intracluster interaction has been handled within the isotropic exchange model; the intercluster one within the molecular field approximation.

The eigenvalues of the isotropic exchange Hamiltonian, for the tetranuclear system

$$\mathcal{H}_{exch} = -J_{\{3CuFe\}}\mathcal{S}_{\{2CuFe\}}\mathcal{S}_{Cu(Mesalen)} \qquad (6)$$

with $J_{\{3CuFe\}}$ equal to the intratetranuclear interaction parameter, $S_{\{2CuFe\}} = {}^3/_2$, and $S_{Cu(Mesalen)} = {}^1/_2$, are shown schematically in diagram III. Zero-field splittings and g factors are associated

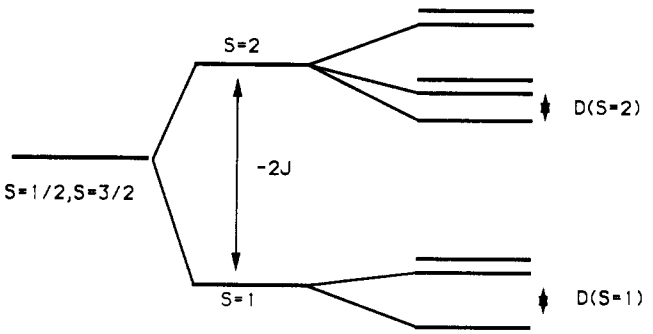

diagram III

with each manifold. The derived susceptibility equation for $S = {}^3/_2$–$S = {}^1/_2$ interacting systems has already been established in the case of localized spins such as in cobalt(II)–copper(II) systems.[13] We have used an identical equation, assuming a localized $S = {}^3/_2$ spin for the trinuclear unit. We have assumed equal g factors and zero-field splittings for each state in order to minimize the number of parameters.

The molecular field approximation[14] shows that the intermolecular coupling can be taken into account by the introduction of the Weiss constant Θ in the susceptibility equation. Such approximation has been demonstrated to be equivalent to the consideration of the intermolecular term $\mathcal{H} = zJ'\mathcal{S}_i\mathcal{S}_j$ in the spin Hamiltonian, with J' denoting the intermolecular exchange parameter and z the number of neighbors, provided the interaction is small.[15]

The temperature dependence of the susceptibility is then expressed by the equation

$$\chi_{\{3CuFe\}} = N\mu_B^2/K(T - \Theta)\{(g^2/4)f(J,D,T)\} \qquad (7)$$

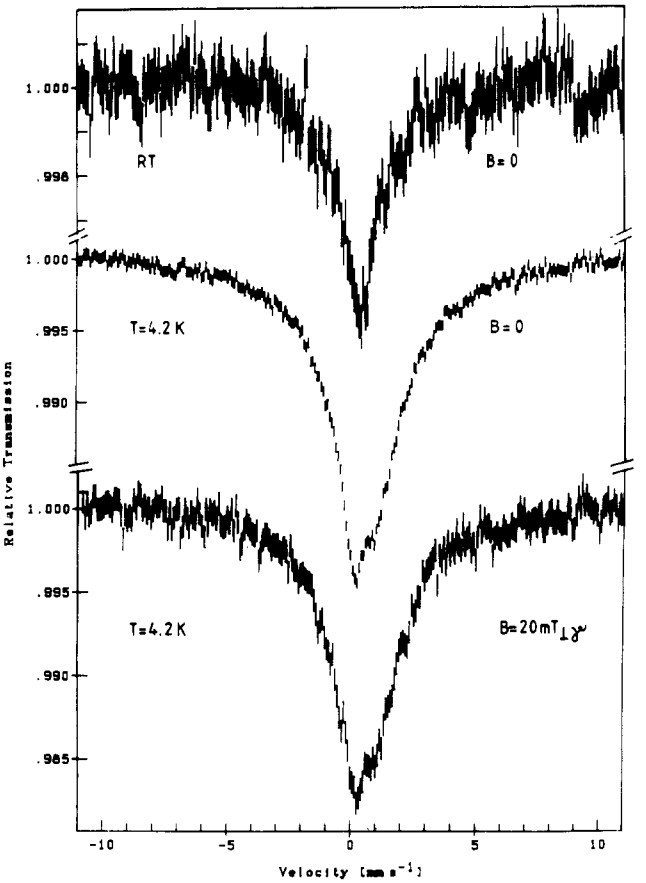

Figure 4. Mössbauer spectra of {2CuFe} taken at 4.2 K and room temperature (RT) in zero magnetic field and under a small field (20 mT) applied perpendicular to the γ-ray at 4.2 K. The broadening of the pattern is due to spin–spin relaxation.

with $f(J,D,T)$ given elsewhere.[13] The fit of the low-temperature susceptibility data to this equation leads to the parameter values

$$J_{\{3CuFe\}} = -3.7\ cm^{-1} \qquad g_{\{3CuFe\}} = 2.25 \qquad D_{\{3CuFe\}} = 1.9\ cm^{-1}$$

$$\Theta = 2.1\ K \qquad R\ \text{factor} = 2 \times 10^{-4}$$

We are aware that these values cannot be ascertained uniquely because of the necessity to adjust several correlated parameters in a narrow range of data. Nevertheless, despite the number of approximations we used, these results associated with the ones obtained in the high-temperature study show consistency, since there is a quite perfect overlap of the corresponding theoretical curves over the range 30–40 K that corresponds to the approximate plateau of the experimental data in Figure 3. The parameter values J and D are larger than those obtained in the Mössbauer study, but, owing to their strong correlation, their ratio $|J/D|$ has to be compared and is found equal to 2 in both studies.

The intercluster interaction, given by Θ, is slightly weaker than the intranuclear interaction, its order of magnitude being in agreement with the structural molecular disposition. Although the molecular field approximation rests on the hypothesis of an intermolecular interaction much weaker than the intramolecular one, it allows us to approach the real structure of the tetranuclear system in which those two interactions should in fact be identical. A model that would explicitly consider the polymeric chain is needed.

Mössbauer Properties. Trinuclear Complex {2CuFe}. Mössbauer spectra in zero field recorded at 4.2 K and at room temperature (Figure 4, top and middle) correspond to those presented in our earlier study.[5] They consist of broad magnetic patterns. A small field (20 mT) applied perpendicular to the γ-ray at 4.2 K in order to stabilize the hyperfine structure by decoupling electronic and nuclear spins as suggested by Afanas'ev and Kagan[16] does not

(13) (a) Lambert, S. L.; Spiro, C. L.; Gagné, R. R.; Hendrickson, D. N. *Inorg. Chem.* **1982**, *21*, 68–72. (b) Morgenstern-Badarau, I.; Cocco, D.; Desideri, A.; Rotilio, G.; Jordanov, J.; Dupre, N. *J. Am. Chem. Soc.* **1986**, *108*, 300–302.

(14) Hatfield, W. E. In *Theory and Applications of Molecular Paramagnetism*; Boudreaux, E. A., Mulay, L. N., Eds.; Wiley: New York, 1976.

(15) Ginsberg, A. P.; Lines, M. E. *Inorg. Chem.* **1972**, *11*, 2289–2290.

(16) Afanas'ev, A. M.; Kagan, Yu. M. *JETP Lett.* **1968**, *8*, 382.

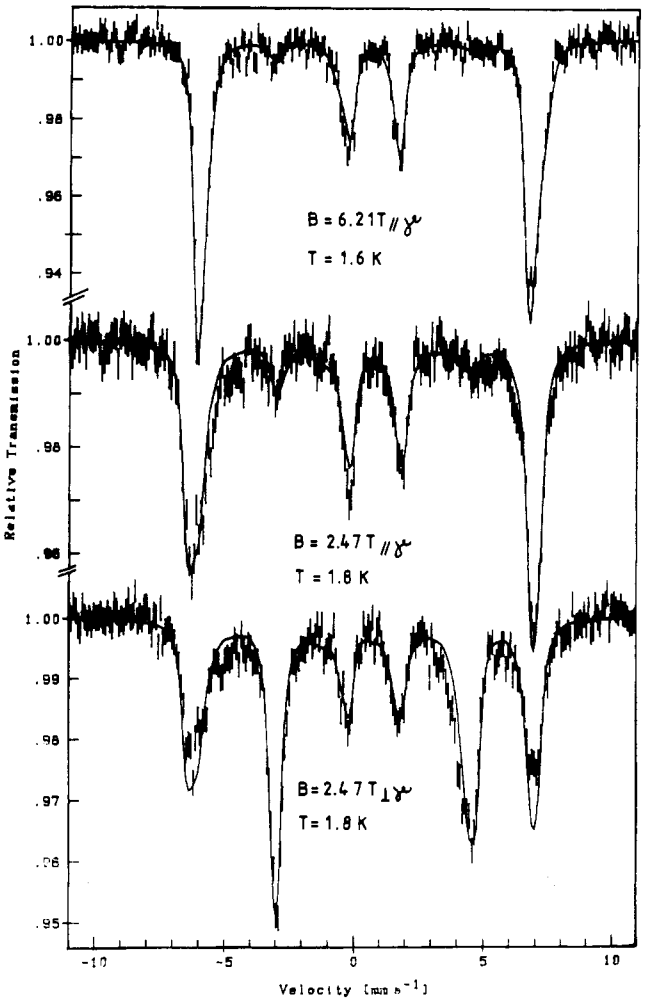

Figure 5. Mössbauer spectra of {2CuFe} at 1.6 K and under 6.21 T applied parallel to the γ-ray and at 1.8 K and under 2.47 T applied parallel as well as perpendicular to the γ-ray.

produce the desired effect (Figure 4, bottom). This means that the broadening of the pattern is not due to random dipolar fields produced by the ions of the surrounding but presumably caused by spin–spin relaxation. Elevation to room temperature is in any case not sufficient to make the relaxation fast enough for the observation of a resolved electric quadrupole doublet. Good spectral resolution is obtained, however, under large applied fields and at temperatures below 2 K (Figure 5). Under these conditions only the ground state of the spin multiplet is populated and cross-relaxation with neighbors in excited states cannot occur. Thus, it is possible to use these spectra in order to parametrize the hyperfine interaction in terms of the spin Hamiltonian formalism[17,18] in the slow-relaxation limit.

From our earlier magnetic susceptibility study,[5] it is known that the $S = {}^3/_2$ ground-state multiplet is well separated in energy from other spin states. Therefore, a spin Hamiltonian for a single $S = {}^3/_2$ system of the form

$$\mathcal{H} = \mathcal{S}(D)\mathcal{S} + \beta\mathcal{S}(g)B + \mathcal{S}(A)\mathcal{I} + \mathcal{H}_Q - g_N\beta_N B\mathcal{I} \quad (8)$$

has been used for the simulation of the Mössbauer spectra recorded at 1.6 K under 6.21 T applied parallel to the γ-ray and at 1.8 K under 2.47 T applied parallel as well as perpendicular to the γ-ray.

The overall magnetic splitting of the high-field (6.21 T) spectrum at 1.6 K is determined by the A tensor. Under this experimental condition only one Zeeman level is populated and therefore the spectral pattern yields no information about the zero-field splitting. From the simulation, it is found that the A tensor might exhibit a slight anisotropy: $A_{xx} = -(30.4 \pm 0.3)$ T, $A_{yy} = -(30.8 \pm 0.3)$ T, $A_{zz} = -(31.2 \pm 0.5)$ T. These results are to be related to the total spin $S = {}^3/_2$. The values relative to the individual iron spin ($S = {}^5/_2$) can be deduced from the vectorial model[19] and are given in Table IV. At moderate applied field (2.47 T) several sublevels are populated even at 1.6 K, the spin-expectation values of which depend on the zero-field-splitting D and the rhombicity E/D with $D = (2D_{zz} - D_{xx} - D_{yy})/2$ and $E = (D_{xx} - D_{yy})/2$. In the slow-relaxation limit, the resulting Mössbauer spectrum is a superposition of the corresponding subspectra. The intensities of the "forbidden" $\Delta m = 0$ transition in the absorption spectra recorded under parallel field are particularly controlled by the size of D because the excited Zeeman levels produce also spin components perpendicular to the γ-ray direction. Values of $D = 1.4$ cm^{-1} and $E/D = 0.1$, the latter being consistent with EPR results, lead to reasonable simulations (solid lines in Figure 5).

Table IV. Fine Structure and Hyperfine Structure Parameters Derived for Complexes {2CuFe} and {3CuFe}

	{2CuFe}	{3CuFe}
δ,[a] mm s^{-1}	0.60 (3)	0.60 (3)[b]
ΔE_Q, mm s^{-1}	1.15 (3)	0.51 (3)[b]
Γ, mm^{-1}	0.30 (3)	0.40 (3)[b]
η, mm^{-1}	0.4 (3)	0.0
D, cm^{-1}	1.4 (2)	0.75 (3)
E/D	0.10 (2)	0.10 (2)
g_x	1.96 (3)	1.96 (3)
g_y	1.96 (3)	1.96 (3)
g_z	1.96 (3)	1.96 (3)
$A_{xx}({}^3/_2)$, T	−30.4 (3)	−29.3 (3)
$A_{xx}({}^5/_2)$, T	−21.7 (2)	−20.9 (2)
$A_{yy}({}^3/_2)$, T	−30.8 (3)	−31.5 (3)
$A_{yy}({}^5/_2)$, T	−22.0 (2)	−22.5 (2)
$A_{zz}({}^3/_2)$, T	−31.2 (5)	−31.8 (5)
$A_{zz}({}^5/_2)$, T	−22.3 (4)	−22.7 (4)
J, cm^{-1}		−1.6 (2)
w_o, s^{-1}	0.26×10^9	2.2×10^9
Euler Angles Taking the D Tensor into the efg Tensor		
α_{efg}, deg	30 (5)	30 (5)
β_{efg}, deg	25 (5)	25 (5)
γ_{efg}, deg	0	0

[a] Relative to α-Fe at room temperature. [b] At 4.2 K.

Information about the magnitude of the efg tensor and its orientation with respect to D was obtained by reproducing the line intensities and broadenings of the spectra recorded under 2.47 T. Special attention has been given to the changes that occur when the field is applied perpendicular to the γ-ray instead of parallel. The values of the Euler angles α and β and for the asymmetry parameter η were finally determined as $(30 \pm 5)°$, $(25 \pm 5)°$, and 0.5 ± 0.1, respectively. The shapes of the calculated spectra are little affected by a modification of the g values. However, we get most satisfactory simulations with values smaller than 2 ($g_x = g_y = g_z = 1.96$). This is qualitatively in agreement with the results that can be derived from the vectorial model.[19]

The fact that we were able to simulate the spectra using a single spin $S = {}^3/_2$ confirms the existence of an antiferromagnetic coupling between iron(III) and the two copper(II) ions as suggested by the earlier susceptibility investigation of the {2CuFe} cluster.[5] With the parameter set derived from the low-temperature spectra assuming static conditions, we were able to simulate the spectra recorded at elevated temperatures by taking properly into account relaxation effects (see below).

Tetranuclear Complex {3CuFe}. The Mössbauer spectra recorded at zero field at different temperatures consist each of a resolved quadrupole doublet. As a representative example, the 4.2 K spectrum is shown in Figure 6. Isomer shift δ, quadrupole splitting ΔE_Q, and line width Γ were obtained from least-squares fits of the spectra using Lorentzian lines. The observed isomer shift of about 0.6 mm s^{-1} and the quadrupole splitting of about

(17) Münck, E.; Champion, P. M. *J. Phys. Colloq.* **1974**, *35*, C6-33.
(18) Münck, E. In *Methods in Enzymology*; Academic Press: New York, 1978.
(19) Chao, C. C. *J. Magn. Reson.* **1973**, *10*, 1–6.

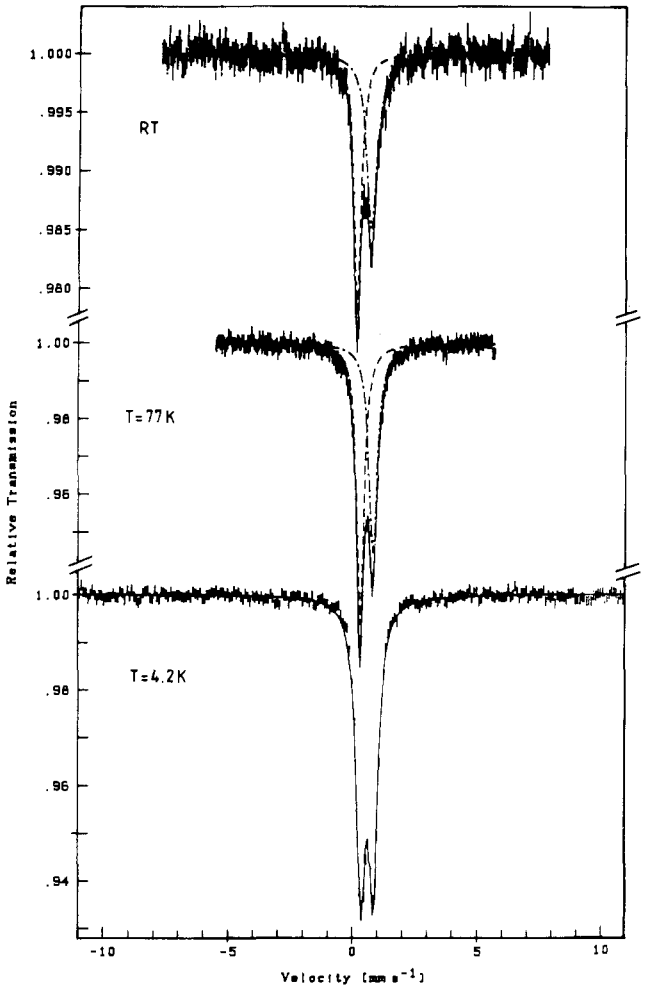

Figure 6. Mössbauer spectra of {3CuFe} taken at 4.2 K, 77 K, and room temperature (RT) in zero magnetic field. The solid lines are the result of least-squares fits to the data assuming Lorentzian lines.

0.5 mm s^{-1}, both at 4.2 K, establish that the material is in the high-spin ferric state.

We have recorded also a series of Mössbauer spectra at 1.5 K under applied fields of 2.47 and 6.21 T. From comparing the hyperfine pattern of the {2CuFe} and the {3CuFe} systems, we deduce that the tetranuclear complex is most likely built up by the known trinuclear complex plus a Cu(Mesalen) monomer with a weak antiferromagnetic coupling between the two due to the following reasons: (i) At 1.5 K under large applied field (6.21 T) the spectrum of {3CuFe} is nearly identical with that of {2CuFe} (Figure 7, right), as it is expected if the coupling is so weak that the field brings about a decoupling. (ii) At 1.5 K and under 2.47 T the effect of the coupling becomes observable through a reduction of the magnetic splitting of {3CuFe}, with respect to {2CuFe} (Figure 7, left), which points to its antiferromagnetic character.

Because the coupling is existent but weak, most of the spectra cannot be simulated by assuming a single spin. In order to analyze the experimental spectra of {3CuFe} in terms of the spin Hamiltonian formalism, we consider {2CuFe} as a system with localized total spin $S = {}^3/_2$ that interacts with the single spin $S = {}^1/_2$ of the Cu(Mesalen) molecule. Therefore, the spin Hamiltonian has been assumed to have the following form:

$$\mathcal{H} = -\mathcal{S}(J)\mathcal{S}' + \mathcal{S}(D)\mathcal{S} + \beta\mathcal{S}(g)B + \mathcal{S}(A)\mathcal{I} + \mathcal{H}_Q - g_N\beta_N B\mathcal{I} \quad (9)$$

Due to the similarity of the spectra obtained from {2CuFe} and {3CuFe} under 6.21 T, the components of the hyperfine tensor (A) derived for {3CuFe} are numerically close to those determined for {2CuFe} (Table IV). The magnetic splitting of the 2.47-T spectra is sensitive to both zero-field-splitting parameter D and spin-coupling constant J. Therefore, it is possible from the simulation of these spectra to derive only an estimate of the ratio $|J/D|$. The simulation of the relaxation spectra recorded at higher temperatures under applied field, as will be described below, was necessary in order to determine D alone. We obtained $D = (0.75 \pm 0.03)$ cm^{-1}. From this value, the magnetic splitting of the two 2.47-T spectra was successfully simulated with an isotropic J of -1.6 cm^{-1}. The asymmetry parameter η turned out to be nearly zero. The g tensor and the orientation of the efg tensor with respect to D were left unchanged in relation to {2CuFe}.

We want to mention that the agreement between the experimental and the simulated spectra using the parameter set given in Table IV is reasonable. Our model assumes an antiferromagnetic spin coupling between two localized spins, i.e., between $S = {}^3/_2$ for the whole {2CuFe} cluster and $S' = {}^1/_2$ for the Cu(Mesalen) monomer. We are aware that this approach cannot be extended continuously to higher temperatures or larger fields. A more general treatment would have to consider each individual spin of the trinuclear cluster and to take into account the couplings within the cluster as well as with the monomer explicitly. This scheme will become even more complicated by the presence of solid-state properties in {3CuFe}.

Spin–Spin Relaxation. As pointed out above, only the spectra recorded below 2 K in moderate and strong applied fields could

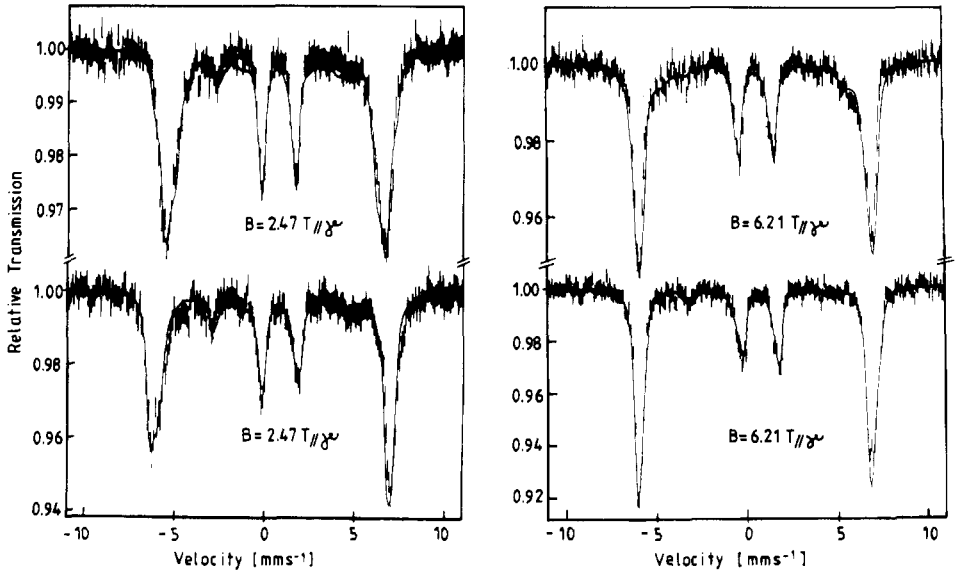

Figure 7. Mössbauer spectra of {2CuFe} (lower one) and {3CuFe} (upper one) at 1.5 K under 2.47 and 6.21 T parallel to the γ-ray.

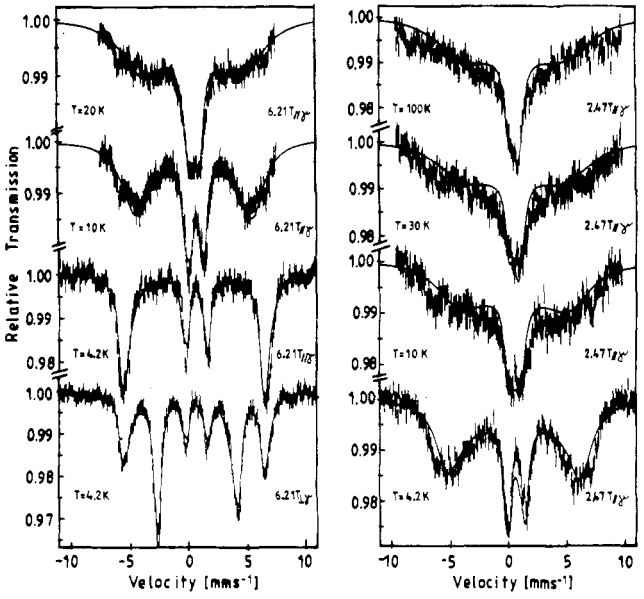

Figure 8. Relaxation spectra of {2CuFe} under 6.21 and 2.47 T in a temperature range between 4.2 and 100 K simulated with the spin-relaxation model using the parameters of Table IV.

be simulated under the assumption that the hyperfine interaction is static in the time scale of the Mössbauer window. At 4.2 K the line shapes change already more or less dramatically depending on the strength of the applied field in a manner that is characteristic for electronic spin relaxation. Because of the relatively high concentration of paramagnetic centers in the materials under study, it is to be expected that spin–spin interaction is responsible for the relaxation.

Spin–spin relaxation is highly sensitive to distances and provides therefore in principle also information about the spatial arrangement of paramagnetic centers. It can be treated in the usual way within the framework of stochastic theories of line shape[20,21] by specifying the transition probabilities between electronic states which generate various hyperfine interactions properly. Since $2\beta B > 2|D|$ for $B > 1.5$ T if $|D| > 1.5$ cm^{-1}, as in the present cases, the Zeeman interaction in an applied field of 2.47 T and even more of 6.21 T is dominant. Thus, the applied field defines the axis of quantization and the substrates of the spin multiplet are rather pure Zeeman states $|SM\rangle$ independent of the orientation of the molecule in the field having sharp spin projections $S_z = M$ in the applied-field direction.

For the transition probabilities between pure Zeeman levels of d^5 ^6S ions due to spin–spin relaxation, Boyle and Gabriel[22] propose the expressions

$$w(M_a \rightarrow M_a + 1) = w_0 \cdot {}^1/_4 |\langle M_a + 1|S_+|M_a\rangle|^2 \sum_{M_b=-S+1}^{S} |\langle M_b - 1|S_-|M_b\rangle|^2 \rho(M_b) \quad (10a)$$

$$w(M_a \rightarrow M_a - 1) = w_0 \cdot {}^1/_4 |\langle M_a - 1|S_-|M_a\rangle|^2 \sum_{M_b=-S}^{S-1} |\langle M_b + 1|S_+|M_b\rangle|^2 \rho(M_b) \quad (10b)$$

where

$$w_0 = 2\pi/\hbar \sum_j (B_{aj} + J_{aj})^2 P_a(E) \quad (11)$$

contains the dipole–dipole and exchange–coupling constants B_{aj} and J_{aj}, respectively, of the Mössbauer ion "a" with all its neighbors "j" as well as its level density $P_a(E)$, while $\rho(M_b)$ are the Boltzmann populations of the magnetic substrates of any neighbor labeled by "b". This model assumes that the transitions are due to an energy-conserving cross-relaxation process with a paramagnetic neighbor ion. The level spacing between all substrates of b is taken equidistant and equal to that of the Mössbauer ion so that a specific transition in a can be induced by any transition in b as inferred by the sum over M_b. This is different from the case where the zero-field splitting is comparable to or even greater than the Zeeman splitting because under that condition only transitions between equivalent pairs of levels can take place and one gets[23]

$$w(M \rightarrow M \pm 1) = w_0 \cdot {}^1/_4 |\langle M \pm 1|S_\pm|M\rangle|^4 \rho(M \pm 1) \quad (12)$$

For the interpretation of our spectra, we have used the Boyle and Gabriel expressions (10a), (10b), and (11), which seemed to come

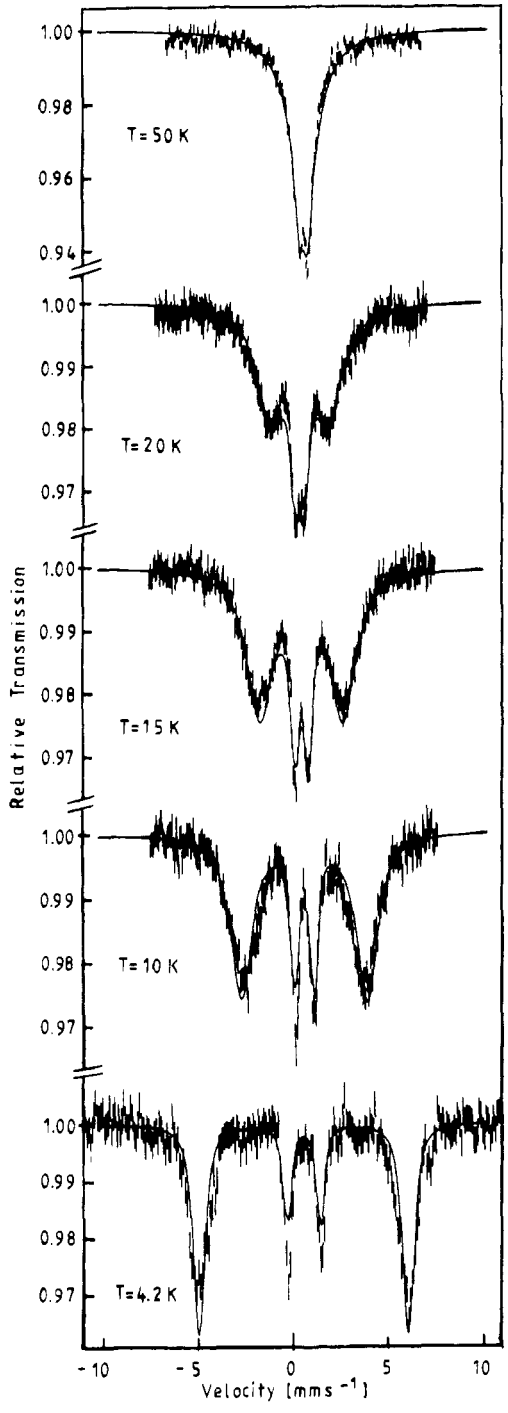

Figure 9. Relaxation spectra of {3CuFe} under 6.21 T parallel to the γ-ray in a temperature range between 4.2 and 50 K simulated with the spin-relaxation model using the parameters of Table IV.

(20) Blume, M. *Phys. Rev.* **1968**, *174*, 351.
(21) (a) Winkler, H.; Schulz, C.; Debrunner, P. G. *Phys. Lett.* **1979**, *69A*, 360. (b) Winkler, H. Habilitation Thesis, University of Hamburg, 1983.
(22) Boyle, A. J. F.; Gabriel, J. R. *Phys. Lett.* **1965**, *19*, 451.
(23) Blume, M. *Phys. Rev. Lett.* **1967**, *18*, 305.

closer to the truth because D is comparatively small.

In the simulations w_0 has been treated as empirical parameter. It is expected to be independent of temperature and field strength as long as the latter is high enough to justify the Boyle and Gabriel model despite of a finite zero-field splitting. Due to the zero-field splitting the level spacings are of course not really equidistant, but this may be compensated in part by an inhomogeneous broadening of the levels. For the spectra of the trinuclear complex recorded under 6.21 and 2.47 T it was indeed possible to get satisfactory simulations for the whole temperature range from 4.2 to 50 K with one single value for w_0. The zero-field splitting, rhombicity, and hyperfine parameters were taken as determined from the low-temperature spectra except that, for the sake of simplicity, the Euler angles α and β of the efg tensor have been disregarded. The solid lines in Figure 8 show the simulations obtained for $S = {}^3/_2$ and the parameters of Table IV with $w_0 = 2.6 \times 10^8\ s^{-1}$. The estimated uncertainty of this value is about 20%.

The relaxation rate in the tetranuclear complex is obviously faster. The solid lines through the spectra in Figure 9 are simulations obtained for $S = {}^3/_2$ and the parameters of Table IV with $w_0 = 2.2 \times 10^9\ s^{-1}$. Direct comparison with the trinuclear complex is possible, since the applied field of 6.21 T is so strong that the spin ${}^1/_2$ of the monomeric Cu(Mesalen) is coupled in a kind of Paschen-Back effect much stronger to the external field than to the spin ${}^3/_2$ of the trimer. The monomer may, however, mediate the cross-relaxation between two trimers, thus enhancing the relaxation rate by about 1 order of magnitude. This finding is not unexpected because it is well-known, e.g. from the work of Bhargava et al.,[24] that the presence of other paramagnetic ions shortens the spin-spin relaxation times substantially. Such an explanation is also consistent with the X-ray structure of the crystalline tetranuclear entity described in the preceding section.

Acknowledgment. This research was supported in part by NATO Research Grant No. 330/87.

Supplementary Material Available: Tables S1 and S2, listing interatomic distances and bond angles for the PF_6 anions and anisotropic thermal parameters (2 pages); a listing of observed and calculated structure factors (19 pages). Ordering information is given on any current masthead page.

(24) Bhargava, S. C.; Knudsen, J. E.; Morup, S. *J. Phys. Chem. Solids* **1979**, *40*, 45.

Contribution from the Departments of Chemistry, Loyola University of Chicago, Chicago, Illinois 60626, and University of Coimbra, 3000 Coimbra, Portugal, and Laboratory of Organic Chemistry, Delft University of Technology, Julianalaan 136, 2628 BL Delft, The Netherlands

Multinuclear NMR Study of the Interaction of the Shift Reagent Lanthanide(III) Bis(triphosphate) with Alkali-Metal Ions in Aqueous Solution and in the Solid State†

Ravichandran Ramasamy,‡,§ Duarte Mota de Freitas,*,‡ Carlos F. G. C. Geraldes,∥ and Joop A. Peters*,⊥

Received January 4, 1991

The paramagnetic ion-induced relaxation rate enhancements of ^6Li in adducts of Li^+ and $Ln(PPP)_2^{7-}$ complexes (Ln = Dy, Tm) in aqueous solution show that up to seven monovalent counterions can coordinate in the second coordination sphere of the Ln(III) ion to the outer oxygens of the triphosphate ligands. However, the pseudocontact ^7Li NMR shift data suggest that in the second coordination sphere some preference of the counterions for the axial region opposite the water ligand may exist. The estimated Ln^{3+}-Li^+ distances range from 5.1 to 5.9 Å for $[Li^+]/[Ln(PPP)_2^{7-}]$ ratios of 0.2-7. This is supported by a two-dimensional nutation spectrum of a polycrystalline sample of $Na_7La(PPP)_2$, which indicates coordination of all Na^+ ions to phosphate oxygens.

Introduction

Several aqueous shift reagents (SRs) for metal cation NMR spectroscopy have been reported.[1-6] They have been shown to be useful in membrane transport biochemistry, for example in studies of alkali-metal ion transport across vesicles[7,8] and red blood cell membranes.[1,9-12] However, only two of them, $Dy(TTHA)^{3-}$ and $Tm(DOTP)^{5-}$, have found useful practical application for perfused heart studies[13,14] and in vivo rat brain ^{23}Na NMR spectroscopy.[15,16] Despite considerable discussion, there seems still to be some controversy regarding the mode of interaction of one of the SRs most widely used for NMR studies in cell systems, namely $Dy(PPP)_2^{7-}$, with alkali-metal ions in aqueous solution.[17-23] Moreover, it has been shown recently that $Dy(PPP)_2^{7-}$ can change ion distribution and transport across red blood cell membranes as well as membrane potential.[24,25] These effects may be related to the mode of binding of alkali metal cations to $Dy(PPP)_2^{7-}$. In this work we further analyze this problem by studying the ^6Li NMR spin-lattice relaxation times of $Dy(PPP)_2^{7-}$ and $Tm(PPP)_2^{7-}$

* Authors to whom correspondence should be addressed.

† Abbreviations used in this paper are as follows: PPP^{5-}, tripolyphosphate; SRs, shift reagents; $TTHA^{6-}$, tetraethylenetetraminehexaacetate; $DOTP^{8-}$, tetraazacyclododecane-*N*,*N*′,*N*″,*N*‴-tetrakis(methanephosphonate); MAS, magic angle spinning; NMR, nuclear magnetic resonance; LnIRE, lanthanide-induced relaxation rate enhancement.

‡ Loyola University.

§ Present address: Department of Chemistry, University of Texas at Dallas, Richardson, TX 75083.

∥ University of Coimbra.

⊥ Delft University of Technology.

(1) Gupta, R. K.; Gupta, P. *J. Magn. Reson.* **1982**, *47*, 344.
(2) Pike, M. M.; Springer, C. S., Jr. *J. Magn. Reson.* **1982**, *46*, 348.
(3) Pike, M. M.; Yarmusch, D.; Balschi, J. A.; Lenkinski, R. E.; Springer, C. S., Jr. *Inorg. Chem.* **1983**, *22*, 2388.
(4) Sherry, A. D.; Malloy, C. R.; Jeffrey, F. M. H.; Cacheris, W. P.; Geraldes, C. F. G. C. *J. Magn. Reson.* **1988**, *76*, 528.
(5) Buster, D. C.; Castro, M. M. C. A.; Geraldes, C. F. G. C.; Malloy, C. R.; Sherry, A. D.; Siemers, T. C. *Magn. Reson. Med.* **1990**, *13*, 239.
(6) Szklaruk, J.; Marecek, J. F.; Springer, A. L.; Springer, C. S., Jr. *Inorg. Chem.* **1990**, *29*, 660.
(7) Pike, M. M.; Simon, S. R.; Balschi, J. A.; Springer, C. S., Jr. *Proc. Natl. Acad. Sci. U.S.A.* **1982**, *79*, 810.
(8) Shinar, H.; Navon, G. *J. Am. Chem. Soc.* **1986**, *108*, 5005.
(9) Brophy, P. J.; Hayer, M. K.; Riddell, F. G. *Biochem. J.* **1983**, *210*, 961.
(10) Ogino, T.; Shulman, G. I.; Avison, M. J.; Gullans, S. R.; den Hollander, J. A.; Shulman, R. G. *Proc. Natl. Acad. Sci. U.S.A.* **1985**, *82*, 1099.
(11) Espanol, M. C.; Mota de Freitas, D. *Inorg. Chem.* **1987**, *26*, 4356.
(12) Pettegrew, J. W.; Post, J. F. M.; Panchalingam, K.; Whiters, G.; Woessner, D. E. *J. Magn. Reson.* **1987**, *71*, 504.
(13) Pike, M. M.; Frazer, J. C.; Dedrick, D. F.; Ingwall, J. S.; Allen, P. D.; Springer, C. S., Jr.; Smith, T. W. *Biophys. J.* **1985**, *48*, 159.
(14) Malloy, C. R.; Buster, D. C.; Castro, M. M. C. A.; Geraldes, C. F. G. C.; Jeffrey, F. M. H.; Sherry, A. D. *Magn. Reson. Med.* **1990**, *15*, 33.
(15) Albert, M. S.; Lee, J.-H.; Springer, C. S., Jr. *Abstracts*, 9th Annual Meeting of the Society of Magnetic Resonance in Medicine, New York, NY, 1990; p 1269.
(16) Naritomi, H.; Kanashiro, M.; Sasaki, M.; Kuribayashi, Y.; Sawada, T. *Biophys. J.* **1987**, *52*, 611.
(17) Chu, S. C.; Pike, M. M.; Fossel, E. T.; Smith, T. W.; Balschi, J. A.; Springer, C. S., Jr. *J. Magn. Reson.* **1984**, *56*, 33.
(18) Nieuwenhuizen, M. S.; Peters, J. A.; Sinnema, A.; Kieboom, A. P. G.; van Bekkum, H. *J. Am. Chem. Soc.* **1985**, *107*, 12.

0020-1669/91/1330-3188$02.50/0